



POLITECNICO
MILANO 1863

**SCUOLA DI INGEGNERIA INDUSTRIALE
E DELL'INFORMAZIONE**



EXECUTIVE SUMMARY OF THE THESIS

Deployment of a CubeSat radiative surface through an autonomous torsional SMA actuator

LAUREA MAGISTRALE IN AERONAUTICAL ENGINEERING - INGEGNERIA AERONAUTICA

Authors: ALBERTO RICCARDO DONATI, FILIPPO CARNIER

Advisor: PROF. PAOLO BETTINI

Co-advisors: DANIELA RIGAMONTI, ELENA VILLA, CRISTIAN FERRETTI

Academic year: 2022-2023

1. Introduction

Initially designed as a learning tool to introduce students to satellite design, CubeSats have proven over time to be a viable alternative to conventional systems, performing the same scientific operations in a considerably smaller volume. Despite their many innovative aspects, the miniaturization of this class of satellites still presents several challenges to overcome. In particular, integrating hardware components in such limited space restricts design flexibility and poses specific issues in developing adequate thermal control systems due to constrained power supplies.

A commonly adopted strategy for thermal management involves deploying radiator panels to dissipate heat generated by the system's internal components via radiation in the space environment. Among the various deployment mechanism solutions, using shape memory alloy actuators could represent a revolutionary choice. SMA can lead to very convenient devices with a significant reduction in mechanical complexity and size and better reliability of the actuation system. Furthermore, focusing on small systems (mini/micro devices), high power-to-weight ratio and low supply voltages are added to their

advantages, providing an excellent technological opportunity to replace conventional electric, pneumatic or hydraulic actuators across all sectors, especially in the space segment.

Most SMA actuators developed for space applications are employed in the form of wires, bars and thin strips, which function by recovering a tensile-kind deformation. The most famous ones include the Lightweight Flexible Solar Array Hinge, an experiment conducted during a Space Shuttle mission in July 1999 which was able to exploit the Shape Memory Effect (SME) of some thin strips to deploy a solar panel [1], and the Mars Pathfinder mission in 1997, which used a NiTi wire actuator to remove the glass cover of some solar cells in order to analyze the deposition of martian dust on them [2].

The following work aims to develop a torsional SMA tubular actuator to be integrated on a 12U CubeSat's thermal fluid loop circuit in order to deploy a radiator panel, thus maintaining the satellite's internal environment within the appropriate temperature ranges. The torsional behavior of SMA actuators is not widely discussed in the literature and presents critical aspects that still require further investigation, such as cycling stability, a crucial property for optimal

integration into a space system.

2. Concept description

In the proposed solution, the actuator exhibits an S-shaped tubular morphology. This choice is influenced by the results of a previous study, which considered various hinge mechanism configurations before concluding that a torsional hinge with a passive segment appears to be the most promising solution. Indeed, it enables the reduction of strain inside the tube, thus providing a greater margin for increasing the circuit piping diameter or applying the solution to more confined spaces [4].

The tubular S-shaped morphology enables the integration of the SMA into a closed-loop liquid circuit, allowing for thermal control operations and panel actuation to coexist within the same element, significantly reducing system complexity. In this approach, the mechanism governing the SMA activation is the same fluid flowing inside the circuit, which experiences localized heating within the satellite due to heat dissipation from internal components and external thermal loads. Through convective heat exchange, the tube, initially deformed in torsion in the martensitic phase with the panel fully closed, generates adequate torque as the SME unfolds, ensuring a 90-degree opening of the radiator element. As the deformation imposed on the tube's central section recovers, the end embedded within the panel is compelled to rotate rigidly, subsequently facilitating the panel's movement (Figure 1). When the thermal loads on the satellite are contained, the circulating fluid remains cold, and the tube stays in the martensitic phase so that the panel remains closed. In this condition, the view factor is minimized, limiting radiative heat rejection. As the thermal load increases, the crystallographic transition in the SMA induces the opening of the radiator, maximizing the view factor and thereby enhancing heat dissipation through radiation.

After the first recovery of the memorized form, neither the return to the low temperature (even below M_f) nor subsequent heating can induce further variations in the shape, until a deformation provided by an external element is set again. The act of returning the SMA actuator to deformed conditions as to be able

to exercise its action again after heating is defined "rearm". Since the actuator is required to operate cyclically depending on the satellite's thermal demands, a rearming strategy must be implemented (for instance, the rearming element can be represented by a torsional spring).

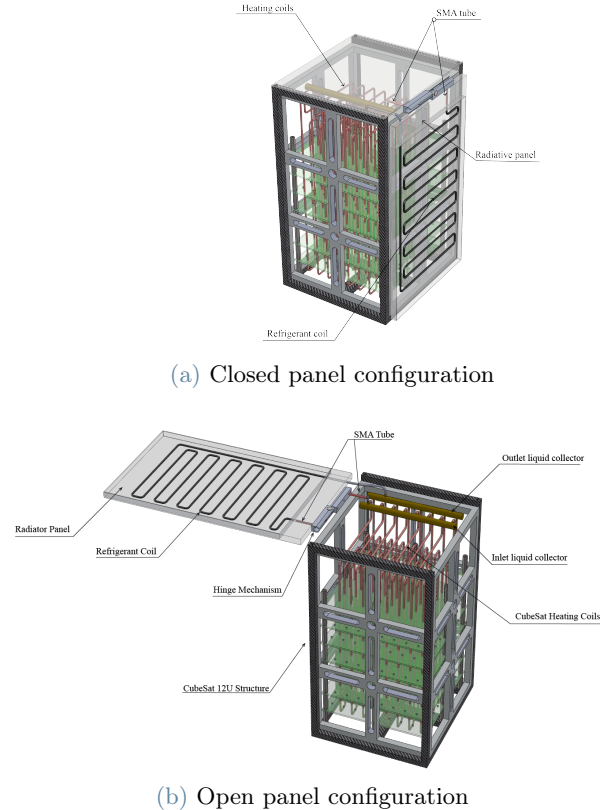


Figure 1

The prospect of utilizing the working fluid itself as a thermal source for SMA activation, without relying on additional energy sources, is highly appealing, especially for systems like CubeSats where the low volume constrains available energy resources. This can be achieved if the panel opening synchronizes with the temperature change and if this change surpasses the final austenite transition temperature (A_f), thereby triggering the activation/recovery process.

3. Manufacturing and thermo-mechanical characterization of the SMA actuator

In the present work, the focus has been placed on the development of an experimental mockup aimed at providing a proof of concept for the

solution just discussed. The apparatus simulates only the fluid heating, and consequently, the functionalities are limited to the single panel opening process. The opening and closing cycles are conducted using manual rearming after adequately cooling the prototype within refrigeration cells.

The prototype design process began with the production of various actuator samples using unprocessed tubes made of NiTi alloy. To date, the NiTi family of alloys exhibits the best functional properties and it is able to withstand high stresses and recover important deformations. NiTi alloy also has other advantages in terms of corrosion resistance, fatigue resistance and biocompatibility, thus making it the preferred material system for most SMA applications considered today [5]. NiTi tubes are commercially available with different diameters (from 0.1 mm to 20 mm and above) and with both pseudoelastic features ($A_f < \text{room temperature}$ and martensite phase stable at low temperatures) and shape memory ($M_f > \text{room temperature}$ and activation temperature over 60°C). Nonetheless, some of the main applications for SMA tubes are in biomedical field, in particular as initial semi-finished product for stent production. For this reason, most of the easily available products have diameters between 2 and 3 mm and pseudoelastic behaviour. Starting from the unprocessed material purchased, which has an outer diameter of 3 mm, a thickness of 0.24 mm, and pseudoelastic properties, it was necessary to implement heat treatments in order to obtain the desired shape and modify the characteristic temperature set to achieve shape memory properties. Thermal treatments result in the generation of numerous precipitates inside the material, compromising the maximum performance that the actuator can provide. Therefore, for future developments, it will be necessary to employ tubes that already exhibit characteristic temperatures suitable for the final application. The design of suitable heat treatments for the development of the prototype was conducted in previous works [3] and has been reproduced here. The tube is firstly inserted into a mold, designed in accordance with the geometry to be imposed on the material, followed by a two-phase furnace heating: a) preheating the tube to a temperature of 565°C and b) maintaining a constant

temperature at that level for 45 minutes. In Figure 2, it is depicted the final result of the process.



Figure 2: Final outcome of tube shaping

To assess transformation temperatures and behavior, DSC tests have been conducted on a single sample. The results reveal that M_f , M_s , A_s , and A_f are -11.99°C , 20.98°C , 20.43°C , and 43.35°C , respectively.

Rotary recovery tests have also been performed to gain a clear understanding of the actuator's performance, particularly in terms of the material's deformation state recovery capacity (Figure 3). The residual rotation detected at the end of each cycle is related to the vertical distance between the initial and final points of the hysteresis curve, indicating a deformation that the material will not be able to recover. This distance increases as the torsional load applied to the tube increases. For torque values greater than 0.07 Nm, the formation of a non-negligible residual deformation was detected.

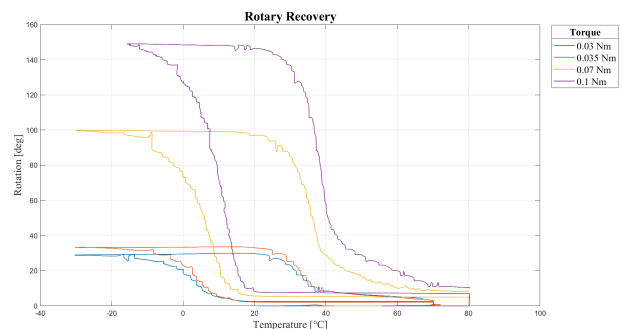


Figure 3: Final outcome of tube shaping

Since in a real application the actuation mech-

anism must provide a certain reliability for the entire duration of the mission, cycling tests have been performed to assess the number of cycles after which a complete recovery of the imposed deformation is no longer guaranteed, due to a permanent modification of the crystalline microstructure of the alloy. The tests were conducted with an applied load of $T = 0,0655\text{Nm}$, as the rotary recovery data indicate that this value represents the minimum load required to impose a 90° rotation on the material in the martensitic phase.

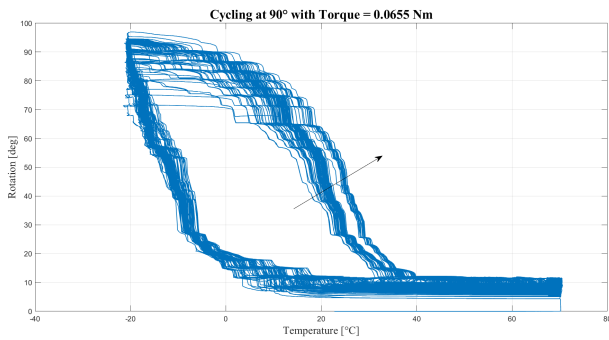


Figure 4: Outcomes of cyclic testing at a set rotational torque of 0.065 Nm

From the cycling tests (Figure 4), it was concluded that after 70 cycles, the material starts to exhibit a destabilization of performance. These results are extremely promising when compared to those of linear actuators with a high degree of precipitates within the matrix, in which the destabilization of shape memory properties emerges after a few cycles.

4. Prototype design and fabrication

A conceptual mockup has been designed (Figure 5) and constructed to evaluate the feasibility of the proposed solution through experimental tests conducted in a terrestrial environment, simulating only the internal heating within the CubeSat. This is because simulating cooling (which occurs in space due to radiation) would have significantly increased the weight and system complexity. Consequently, no rearming mechanism has been implemented. As a result, after each opening process, the system must be cooled inside refrigerators and manually rearmed.

The prototype features a liquid fluid loop inte-

grated into a fixed frame, with dimensions identical to those of a 12U CubeSat structure, and a 3D printed frame free to rotate, representing the radiator panel.

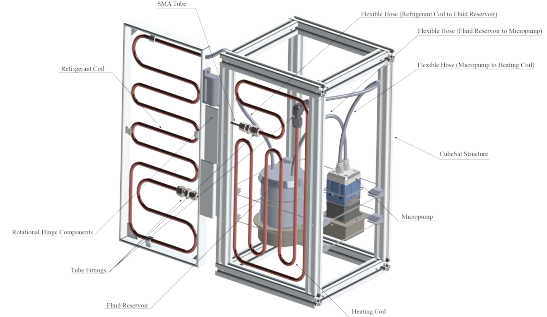


Figure 5: 3D visualization of the realized experimental Mockup

The actuator is housed inside a hinge mechanism necessary to ensure the alignment of the tube to the desired axis of rotation for the panel deployment and its connection to the fixed frame. The hinge consists of two pairs of specular elements (Figure 6), which reproduce the geometry of the mold used for the actuator production, and a fifth element necessary to keep the panel aligned, which would otherwise bend due to gravity.

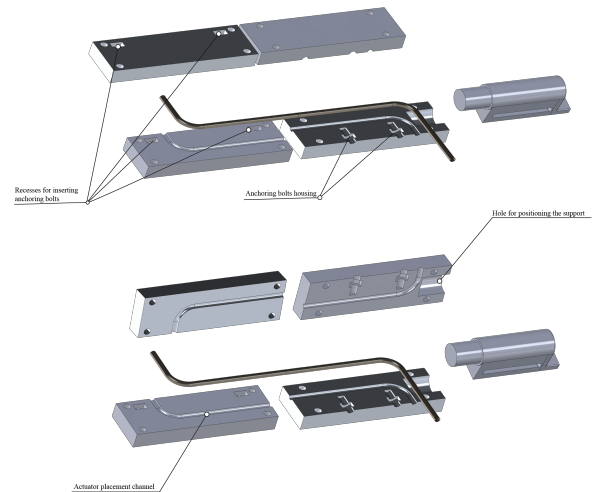


Figure 6: 3D model and exploded view of the ASA Hinge Mechanism

After the assembly, the two pairs of specular counterparts create two distinct elements, one intended to be attached to the fixed frame and the other to the mobile frame, both capable of rotating with respect to each other. Initially, the tube is placed on one half of the mechanism in

the martensitic phase, then the other missing elements are secured to their respective specular counterparts using threaded connections with removable nuts.

The two components are then forced to rotate relative to each other by 90° (in reality, it is necessary to exceed this value due to the elastic recovery of the SMA), thereby generating a torsional stress state in the central section of the tube and thus preloading it in order to mount the panel in a closed configuration. Subsequently, each element is connected to the corresponding frame, and finally, the support element for the panel is inserted and mounted onto the panel itself.

The liquid fluid loop consists of two copper serpentines, each one connected to an end of the actuator, positioned respectively inside the CubeSat structure and the panel. The circulation of the liquid is mediated by a micropump, in turn, connected to the serpentines via PTFE flexible hoses that close the loop. The connections between the various circuit components are hermetically sealed since, with NiTi alloy, the only type of constraint employable is mechanical. The serpentine in the fixed frame is coated with a constantan electrical resistance wire to simulate the liquid heating process (in this case, a 99.9% Propylene Glycol solution was used). A fluid reservoir is also present to prevent excessive pressure increases due to liquid heating. The sizing of the two coils was carried out, taking into account the available space for their housing, while simultaneously trying to maximize the development of the path to control the internal liquid temperature as much as possible, preventing the formation of a two-phase flow. The longer the two components are, the longer the time the working fluid has to dissipate the absorbed heat in the external environment before encountering the heating process upstream of the NiTiNol tube again.

The micropump and the electrical power to be dissipated were chosen based on the numerical results obtained from various CFD simulations, evaluating whether the pressure losses were manageable by the device and whether the convective processes were able to heat the tube beyond A_f . Figure 7 depicts the prototype once assembled.



Figure 7: Global view of the prototype

5. Test results

A test of the prototype was conducted to demonstrate the functionality of the design (Figure 8). The test started with the prototype at room temperature with the SMA tube already in the armed configuration (i.e., panel closed). The micropump was switched on and controlled remotely using a dedicated driver and software. The circulating liquid was heated at the internal coil within the fixed frame using an electric resistance wire, wrapped upstream of the actuator's inlet section, powered to dissipate 400W due to the Joule effect.

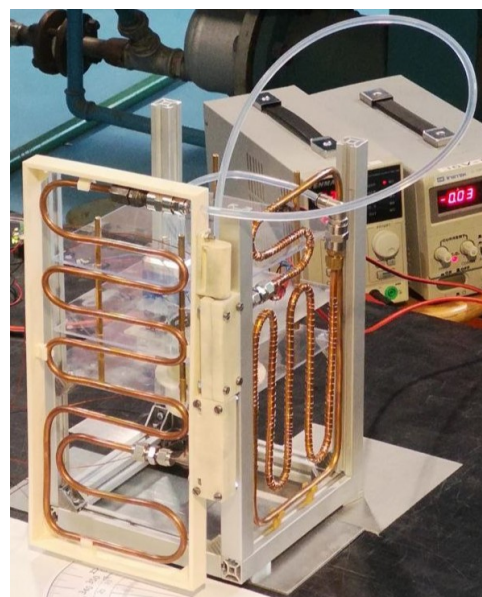


Figure 8: Testing the prototype

The entire process was monitored by a FLIR infrared thermal camera and two thermocouples, positioned at the inlet and outlet sections of the tube, in order to evaluate whether the system's heating was adequate for the purposes of the experimental campaign. The angles reached were measured using a graduated scale located beneath the panel.

The heating proved to be adequate, allowing the tube to reach temperatures suitable for complete austenitization of the alloy. As a result, the panel achieved a rotation of 85° in 155 seconds from the time the current supply was turned on, as shown in Figure 9.

Figure 10 shows a thermal image of the prototype taken by the infrared camera during the heating process after 87 seconds from power supply activation.

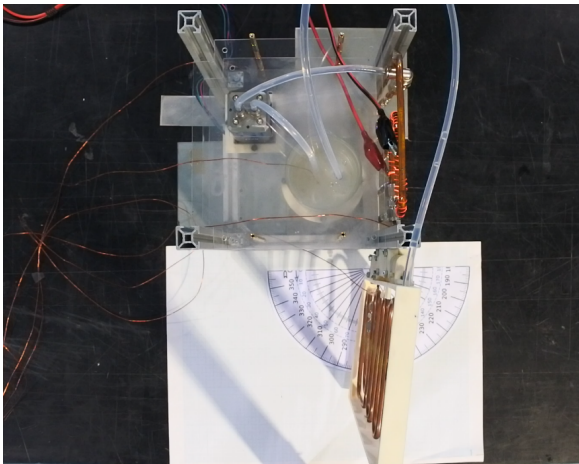


Figure 9: Top view: final angle of 85° achieved

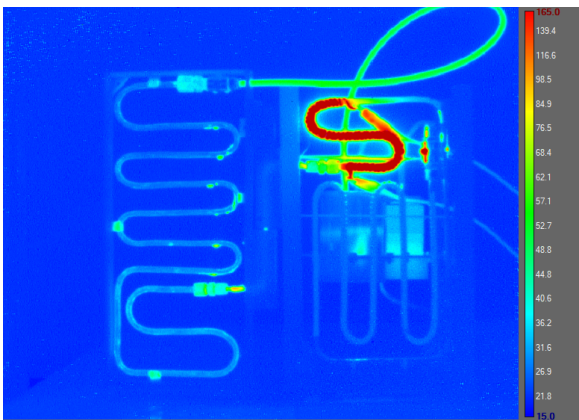


Figure 10: Thermal camera results

Figure 11 shows the temperature trends, detected by the thermocouples, at the inlet and

outlet sections of the actuator. The maximum measured temperatures are $T_{inlet} = 87^\circ C$ and $T_{outlet} = 80^\circ C$. These values are higher than the A_f obtained from the DSC, as the material, in the presence of resistant load, requires more intense heating processes for austenitization.

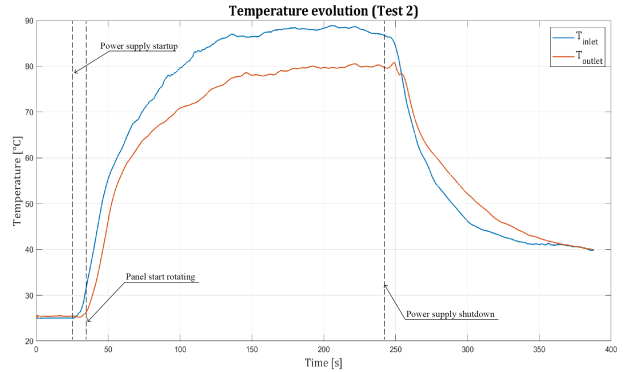


Figure 11: Temperature evolution at the inlet and outlet section of the NitiNol tube

Figure 12 depicts the panel's rotation achieved as the temperature of the tube's outlet sections increases. The opening process, as highlighted, is structured into two main phases. In the first phase, which lasted 7 seconds, the panel reached a 72° rotation. This was followed by a much slower and more controlled development, in which the system stabilized at the maximum rotation angle after 140 seconds. The dual nature of the phenomenon's dynamics depends on the intrinsic characteristics typical of the austenitic transformation process of precipitate-filled alloys. In these materials, in fact, recovery of most of the imposed deformation is observed within a narrow temperature range, followed by the accomplishment of the remaining part of the deformation in a wider range.

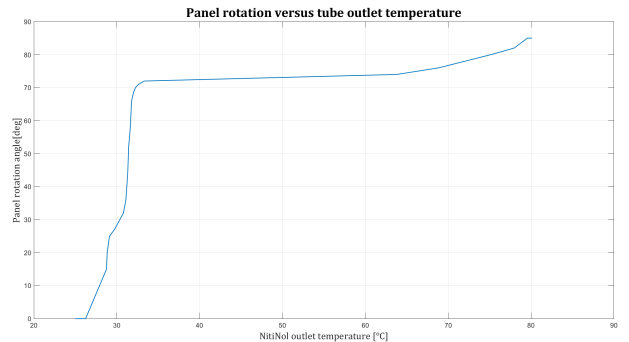


Figure 12: Panel rotation versus tube outlet temperature

The inability to reach a fully open position (i.e., 90° of rotation) is related to the thermal treatments the material underwent. These treatments lead to the formation of precipitates, which compromise the macroscopic recovery of the imposed deformation state during the development of the shape memory effect at the material level.

6. Conclusions

The presented work aims to provide a proof of concept on the feasibility of developing a torsional tubular SMA actuator, which is activated by the internal circulation of a fluid heated to an appropriate temperature. The goal is to integrate this actuator into a 12U CubeSat's thermal fluid loop circuit for the purpose of deploying a radiator panel to 90° angle of rotation.

The actuator geometry relied on previous works' results which indicated that a configuration with an S-shaped torsional hinge seemed to be the most promising solution for the system under development.

The fabrication process started with the production of various actuator samples using precursor tubes for stents, made of NiTi alloy, due to the purchasing easiness. The outer diameter of these tubes is 3 mm and the wall thickness is 0.24 mm. Since these precursor tubes exhibited pseudoelastic behavior, it was deemed necessary to implement thermal treatments in order to obtain the desired morphology and shape memory features.

Torsion tests demonstrated that significant rotations could be achieved at low strain/stress levels, highlighting the suitability of this approach for the 90-degree deployment of a radiating panel on a small satellite. Moreover, cycling tests revealed that, despite the high degree of precipitates within the matrix, the material's stability is ensured for approximately 70 cycles. This result is particularly noteworthy, as it is well known that linear SMA actuators with high precipitate content tend to become unstable much earlier. Consequently, it has been shown that the choice to implement a torsion-based actuation system can be considered highly valid.

Subsequently, a prototype was designed and developed to assess the feasibility of employing the actuator in a real satellite operational context.

The prototype's components were selected or developed to maintain dimensional consistency with the standards of a 12U CubeSat. The system was then tested in a terrestrial environment, yielding highly interesting results, as the panel reached an angle of 85° within a relatively short time. The incomplete achievement of the desired rotation can be attributed to the high concentration of precipitates in the actuator, which compromises its maximum attainable performance. Nevertheless, these results are extremely promising, as, even with this non-optimal material, a comprehensive feasibility study of the system to be developed was provided, demonstrating a solid foundation for reliability.

The work will encompass the following phases: integration of a cooling simulation system into the prototype, development of an appropriate reset mechanism, and the utilization of a suitable shape memory alloy for the final application (i.e., with a limited concentration of precipitates and appropriate characteristic temperatures).

References

- [1] Darren J Hartl and Dimitris C Lagoudas. Aerospace applications of shape memory alloys. *Proceedings of the Institution of Mechanical Engineers, Part G: Journal of Aerospace Engineering*, 221(4):535–552, 2007.
- [2] Phillip P Jenkins and Geoffrey A Landis. A rotating arm using shape-memory alloy. In *NASA. Johnson Space Center, the 29th Aerospace Mechanisms Symposium*, 1995.
- [3] E Redaelli. Development of a sma-based torsional hinge for radiative surface deployment, 2020-2021.
- [4] D Rigamonti, P Bettini, L Di Landro, and G Sala. Development of a smart-hinge based on shape memory alloys for space applications. In *25th Conference of the Italian Association of Aeronautics and Astronautics (AIDAA 2019)*, pages 1719–1742. AIDAA, 2019.
- [5] John A Shaw et al. Tips and tricks for characterizing shape memory alloy wire: part 1-differential scanning calorimetry and basic phenomena. 2008.